Journal of Power Sources 185 (2008) 1519–1523

Contents lists available at ScienceDirect

Journal of Power Sources

journal homepage: www.elsevier.com/locate/jpowsour

Short communication

Study on microstructure and electrochemical performance of $La_{0.7}Mg_{0.3}(Ni_{0.9}Co_{0.1})_x$ hydrogen storage alloys

L.F. Cheng[a,*], R.B. Wang[b], Z.H. Pu[b], Z.L. Li[b], D.N. He[a], B.J. Xia[b]

[a] National Engineering and Research Center for Nanotechnology, 28 Jiangchuan East Road, Shanghai 200241, China
[b] Shanghai Institute of Micro-system and Information Technology, Chinese Academy of Sciences, Shanghai 200050, China

ARTICLE INFO

Article history:
Received 23 May 2008
Received in revised form 17 July 2008
Accepted 6 August 2008
Available online 14 August 2008

Keywords:
Hydrogen storage alloy
La_2Ni_7 phase
Electrochemical properties

ABSTRACT

Hydrogen storage alloys $La_{0.7}Mg_{0.3}(Ni_{0.9}Co_{0.1})_x$ (x = 3.0, 3.1, 3.3, 3.4, 3.5, 3.7 and 3.8) were prepared by inductive melting followed by annealing treatment at 1173 K for 6 h. The effects of the stoichiometry (x) on the structural and electrochemical characteristics of the alloys were investigated systematically. X-ray diffraction (XRD), optical morphology and energy dispersive spectrometry (EDS) analyses showed that these alloys have a multiphase structure which consists of a (La, Mg)Ni_3 phase with the $PuNi_3$-type rhombohedral structure, a $LaNi_5$ phase with the $CaCu_5$-type hexagonal structure and a (La, Mg)$_2Ni_7$ phase with the Ce_2Ni_7-type hexagonal structure. The main phase of the alloys with x = 3.0 and 3.1 is (La, Mg)Ni_3 phase ($PuNi_3$-type structure), the main phase of the alloys with x = 3.3, 3.4 and 3.5 is (La, Mg)$_2Ni_7$ phase (Ce_2Ni_7-type structure), and the main phase of the alloys with x = 3.7 and 3.8 is $LaNi_5$ phase ($CaCu_5$-type structure). Moreover, the lattice parameters of the (La, Mg)Ni_3 phase, (La, Mg)$_2Ni_7$ phase and $LaNi_5$ phase decrease monotonously with the increase of the value x. The electrochemical analysis shows that the maximum discharge capacity increases from 356.6 mA h g^{-1} (x = 3.0) to 392.1 mA h g^{-1} (x = 3.5) and then decreases to 344.1 mA h g^{-1} (x = 3.8), and the alloys exhibit good cycling stability. As the discharge current density is 3000 mA g^{-1}, the high-rate dischargeability (HRD) increases from 30.1% (x = 3.0) to 56.1% (x = 3.8). The low temperature dischargeability (LTD) increases from 24.3% (x = 3.0) to 58.96% (x = 3.7) and then decreases to 48.1% (x = 3.8).

1. Introduction

Among the different ways to store hydrogen, absorption in solid is very attractive since it allows safe storage at the pressure and temperature close to ambient conditions. Various metals and alloys are able to absorb large quantities of hydrogen [1–3]. Among them, intermetallic compounds play a very important role on developing hydrogen-absorbing alloys. Series of metal hydride electrode materials have been developed [4–6], including the rare earth-based AB_5-type alloys, the AB_2-type Laves phase alloys, the V-based solid solution alloys, and the Mg-based alloys. To date, two types of electrode alloys, namely the AB_5- and AB_2-type alloys have been extensively studied and used for commercial batteries [7,8]. However, the AB_5-type alloys have only limited capacity, and the AB_2-type alloys suffer from slow activation and relatively low rate capacity.

$RMgM_n$ ($3 \le n < 5$) (R = rare earth, M = transition metal)-type intermetallic compounds with various stacking structures are currently attracting increasing attention in view of their potential application as new hydrogen-absorbing materials. Several systems with $PuNi_3$-type superstructure, such as La–Mg–Ni–Co, had been studied as negative electrode [9–11]. Superstructure La–Mg–Ni-type hydrogen storage alloy is formed by assembling binary compounds of AB_5 ($CaCu_5$ phase) and AB_2 (Laves phase) units in terms of a certain rule along the c-axis. They crystallize either into the rhombohedral structure of $PuNi_3$-type ($R\bar{3}m$ space group) or into the hexagonal Ce_2Ni_7-type structure ($P6_3/mmc$ space group) which differ only in long range stacking arrangement. From this point of view, the structure can be regarded as intergrowth between AB_5 and AB_2 units following the scheme: $AB_5 + 2AB_2 = 3AB_3$, $3AB_5 + 4AB_2 = A_7B_{23}$ ($AB_{3.3}$), $AB_5 + AB_2 = A_2B_7$ ($AB_{3.5}$), $9AB_5 + 6AB_2 = 3A_5B_{19}$ ($AB_{3.8}$), which is the reason why we call La–Mg–Ni-type hydrogen storage alloy as super-lattices hydrogen storage alloy [1,12,13]. As to their electrochemical hydrogen storage, some researchers reported the discharge capacity of the $La_{0.7}Mg_{0.3}Ni_{2.8}Co_{0.5}$ alloy reached 380–410 mA h g^{-1}, with fairly good cyclic stability within 30 cycles [12,14–16].

However, the overall electrochemical properties of the super-lattices La–Mg–Ni-type hydrogen storage alloy should be further improved for their practical application. Therefore, further investi-

* Corresponding author. Tel.: +86 21 34291286; fax: +86 21 34291121.
E-mail address: chenglifang@china.com.cn (L.F. Cheng).

0378-7753/$ – see front matter © 2008 Elsevier B.V. All rights reserved.
doi:10.1016/j.jpowsour.2008.08.005

gations for improving the cyclic stability are crucial for the further development of this alloy system. It is well known that the stoichiometry (x) of AB_x is the key to improve the electrochemical properties [17] including the maximum discharge capacity, the activation, the high-rate dischargeability (HRD), low temperature dischargeability (LTD) and the cyclic stability of the alloy electrodes. In this investigation, the structure and electrochemical properties of the $La_{0.7}Mg_{0.3}(Ni_{0.9}Co_{0.1})_x$ hydrogen storage alloys were studied systematically.

2. Experimental details

2.1. Preparation of the alloys

The chemical compositions of the investigated alloys were $La_{0.7}Mg_{0.3}(Ni_{0.9}Co_{0.1})_x$. The purity of all the component metal (La, Mg, Ni and Co) is at least 99%. The alloy samples were prepared by induction levitation melting of the constituent metals on a water-cooled copper crucible under argon atmosphere for about 2 min in melting time. The ingot was turned over and remelted three times for homogeneity. Then the obtained cast ingots were annealed at the constant temperature of 1173 K for 6 h under vacuum after a heating rate of about 10 K min^{-1} and then cooled to room temperature with annealing furnace by itself. Then, the alloy sample was mechanically crushed and ground into powders of 400–200 mesh size for both X-ray diffraction (XRD) and electrochemical analysis.

2.2. Microstructure determination and morphology observation

The samples were encapsulated in epoxy resin for polishing. The sample surface thus prepared was etched with a 60% HF solution. The morphologies of the alloys were observed by optical microscope and micro-area component was analyzed by energy dispersive spectrometry (EDS) of INCAX-sight 7200. The phase structures of the alloys were determined by XRD diffractometer of D/max/2000. The diffraction was performed with Cu $K\alpha_1$ radiation filtered by graphite. The experimental parameters were 40 mA, 40 kV and 4° min^{-1}.

2.3. Electrode preparation and electrochemical measurements

All test electrodes were prepared by cold pressing a mixture of 0.3 g alloy powder and 1.2 g carbonyl nickel powder to pellets of 15 mm in diameter and about 1 mm in thickness under a pressure of 15 MPa. The alloy pellet was then interposed between two sintered $NiOOH/Ni(OH)_2$ counter electrode. The electrodes were immersed in 6 M KOH solution for 4 h in order to wet thoroughly the electrodes before the electrochemical measurement. The electrochemical measurements were conducted at 293 K in a two-electrode electrolytic cell consisting of a working electrode (MH electrode), and a $NiOOH/Ni(OH)_2$ counter electrode, immersed in the electrolyte of 6 M KOH solution. The discharge capacity was determined galvanostatically by using an automatic charge/discharge unit. Each electrode was charged at 60 mA g^{-1} for 7.5 h, followed by a 5 min rest, and then discharged at 60 mA g^{-1} to cut-off potential of 1 V versus the counter electrode. For cycling test, the activated electrode was charged each time at 300 mA g^{-1} for 1.3 h and discharged at 300 mA g^{-1} to 1 V versus the counter electrode. The high-rate dischargeability (HRD 3000) was evaluated from the ratio of the discharge capacity measured at 3000 mA g^{-1} (C_{3000}) to the total capacity defined as the sum of C_{3000} and C^*_{60} which was the additional capacity measured subsequently at 60 mA g^{-1} after C_{3000} was measured. The low temperature dischargeability was measured after laying the cell in a low temperature (233 K) equipment (WGD7005) for 12 h. In the HRD and LTD discharge process, the cells were discharged to cut-off voltage of 0.8 V.

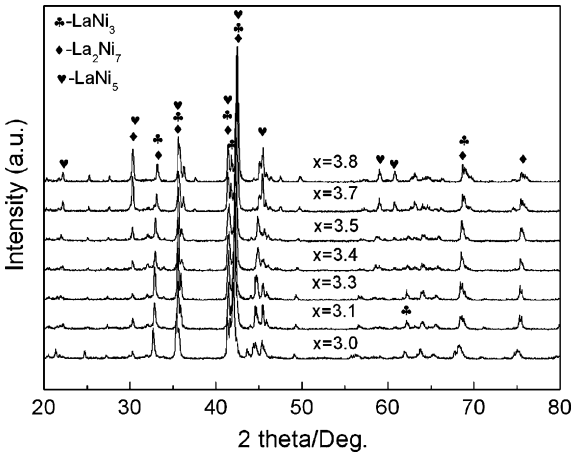

Fig. 1. X-ray diffraction patterns of the $La_{0.7}Mg_{0.3}(Ni_{0.9}Co_{0.1})_x$ alloys.

3. Results and discussion

3.1. Phase structure of the alloys

The XRD patterns of the $La_{0.7}Mg_{0.3}(Ni_{0.9}Co_{0.1})_x$ alloys were shown in Fig. 1. The alloys have a multiphase structure, composed of (La, Mg)Ni_3 phase with $PuNi_3$-type rhombohedral structure, $LaNi_5$ phase with $CaCu_5$-type hexagonal structure, and $(La, Mg)_2Ni_7$ phase with Ce_2Ni_7-type hexagonal structure. When $x = 3.0$ and 3.1, the main phase of the alloys is (La, Mg)Ni_3 phase ($PuNi_3$-type structure). When $x = 3.3$, 3.4 and 3.5 the main phase of the alloys is $(La, Mg)_2Ni_7$ phase (Ce_2Ni_7-type structure). However, when $x = 3.7$ and 3.8 the main phase of the alloys is $LaNi_5$ phase ($CaCu_5$-type structure).

From Table 1 the a-axis and the c-axis of (La, Mg)Ni_3 phase, $(La, Mg)_2Ni_7$ phase and $LaNi_5$ phase are all decreased with the increase of the value x.

Table 1
The lattice parameters of the (La, Mg)Ni_3 phase, $(La, Mg)_2Ni_7$ phase and $(La, Mg)_2Ni_7$ phase in $La_{0.7}Mg_{0.3}(Ni_{0.9}Co_{0.1})_x$

x	(La, Mg)Ni_3 phase ($PuNi_3$-type)		$(La, Mg)_2Ni_7$ phase (Ce_2Ni_7-type)		$LaNi_5$ phase ($CaCu_5$-type)	
	a (Å)	c (Å)	a (Å)	c (Å)	a (Å)	c (Å)
3.0	5.062	24.528				
3.1	5.050	24.505	4.995	24.542		
3.3	5.024	24.456	4.973	24.504		
3.4	5.014	24.434	4.961	24.485		
3.5	5.006	24.416	4.95	24.463		
3.7			4.922	24.414	5.031	4.002
3.8			4.917	24.399	5.026	3.996

3.2. Microstructure of the alloys

The morphologies of the alloys observed by optical microscope are shown in Fig. 2. All alloys exhibit multiphase structure and possess a discrete precipitate morphology. The results obtained by energy dispersive spectrometry indicate that all the alloys mainly consist of the (La, Mg)Ni_3 phase (black dot regions in Fig. 2 (x = 3.0 and 3.1)), (La, Mg)$_2Ni_7$ phase (black regions in Fig. 2 (x = 3.3, 3.4, and 3.5)) and $LaNi_5$ phase (white grey regions in Fig. 2 (x = 3.7 and 3.8)). With the increase of the value x, the amount of the (La, Mg)$_2Ni_7$ phases first increase and then decrease. Fig. 2 shows the coarse grains and inhomogeneity of the alloys. It is noticed that

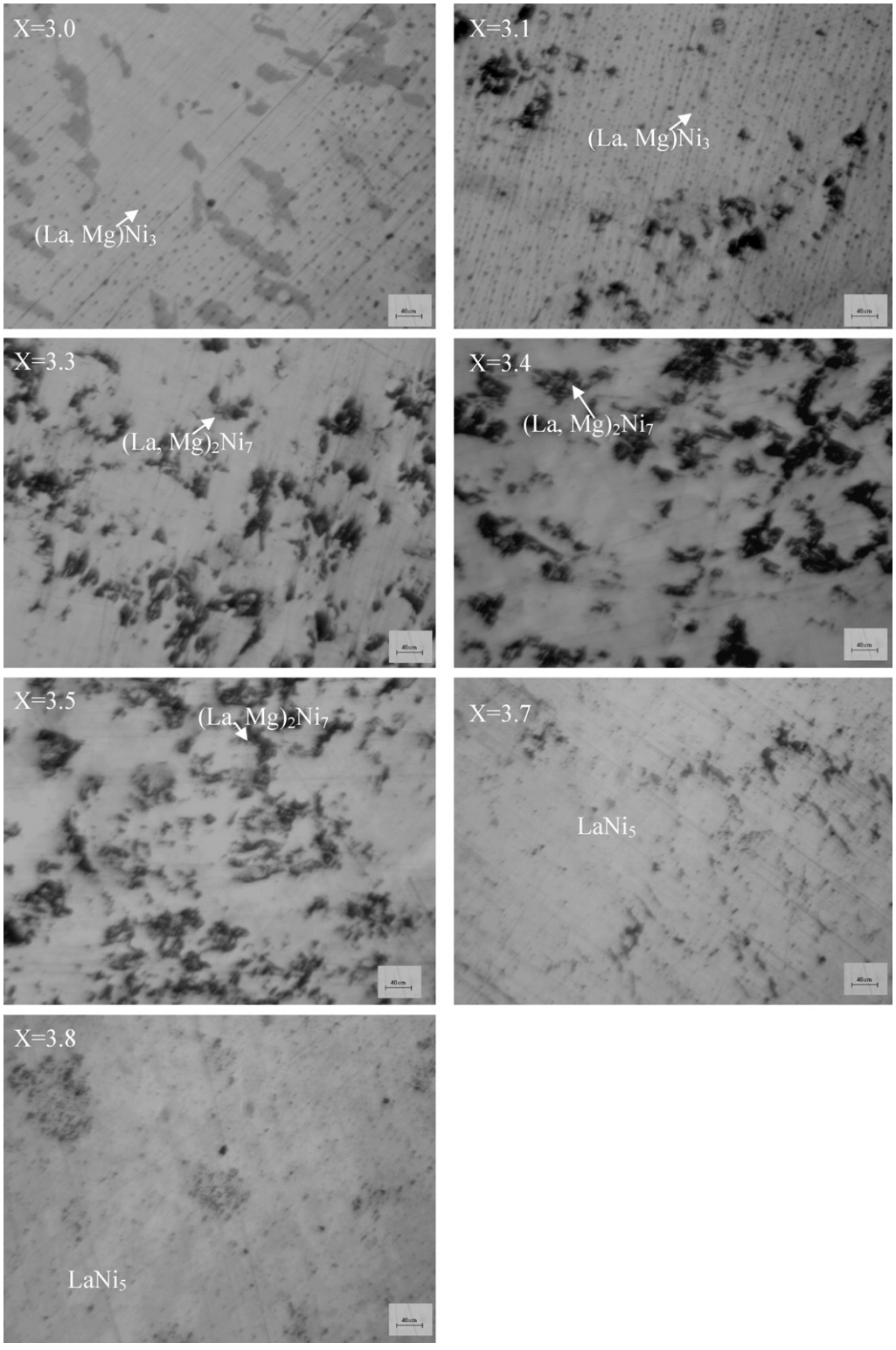

Fig. 2. Optical morphologies of the alloys.

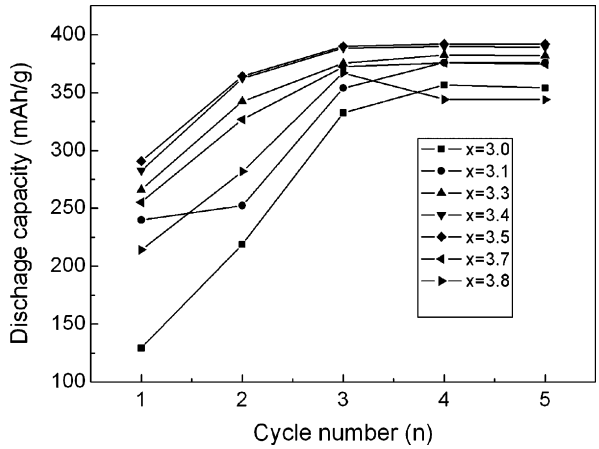

Fig. 3. The activation curves of the $La_{0.7}Mg_{0.3}(Ni_{0.9}Co_{0.1})_x$ alloy electrodes at 293 K.

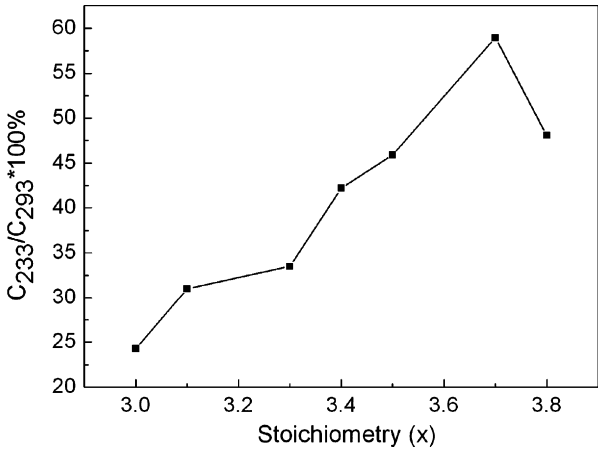

Fig. 5. LTD of $La_{0.7}Mg_{0.3}(Ni_{0.9}Co_{0.1})_x$ alloys electrode.

the grain sizes of the alloys significantly change and the crystal structure changes from round to columnar and then to round with the increase of the value *x*. Stacking structure and electrode properties of the RE–Mg–Ni-based type alloys would be dependent on their elemental composition. The fact that the alloys electrode have good properties could be mainly ascribed to its multiphase structure, because the phase boundary can decrease the lattice distortion and strain energy formed in the process of charging [18,19].

3.3. Electrochemical characteristics

Fig. 3 shows the activation curves of $La_{0.7}Mg_{0.3}(Ni_{0.9}Co_{0.1})_x$ alloy electrodes at 293 K. It can be seen that all the alloys studied are fully activated within three cycles, which would make them attractive in practical applications. The maximum discharge capacity of the alloy electrodes increases from 356.6 mA h g^{-1} ($x = 3.0$) to 392.1 mA h g^{-1} ($x = 3.5$) and then decreases to 344.1 mA h g^{-1} ($x = 3.8$). The discharge capacity of the $La_{0.7}Mg_{0.3}(Ni_{0.9}Co_{0.1})_{3.5}$ alloy reaches 392 mA h g^{-1}, which is much higher than that of commercial AB_5 alloy. This is because that (La, Mg)Ni_3 and (La, Mg)$_2Ni_7$ phases have higher discharge capacity than $LaNi_5$-type alloys [18].

Fig. 4 shows the high-rate dischargeability of $La_{0.7}Mg_{0.3}(Ni_{0.9}Co_{0.1})_x$ alloys. HRD can be calculated by the following expression:

$$\text{HRD}\,(\%) = \frac{C_{3000}}{C_{60}} \times 100 \quad (1)$$

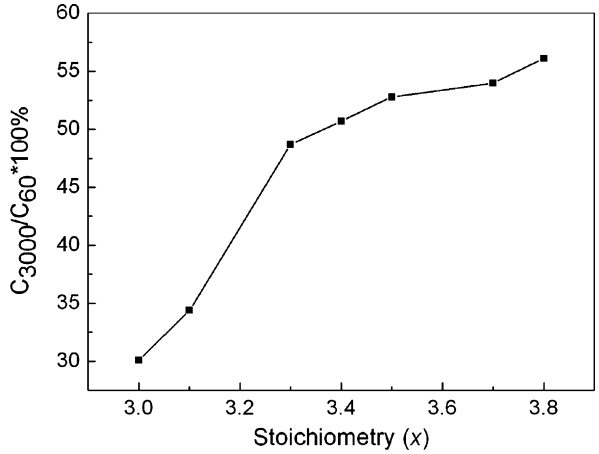

Fig. 4. HRD curve of the $La_{0.7}Mg_{0.3}(Ni_{0.9}Co_{0.1})_x$ alloys.

where C_{3000} is the discharge capacity at current density 3000 mA g^{-1} while C_{60} is the discharge capacity at 60 mA g^{-1}. It can be seen that as the value of *x* increases, the HRD of the alloy electrodes increases from 30.1% ($x = 3.0$) to 56.1% ($x = 3.8$). The HRD is dependent on two factors, namely hydrogen diffusion in the bulk of the alloy and the charge-transfer at the surface of the alloy electrode [20]. It is well known that the elemental Ni has good electro-catalytic activity and the increase of Ni content in the alloy because of increase in the B-site stoichiometry is believed beneficial to the HRD improvement. In addition, the presence of multiphase interfaces provides channels for hydrogen diffusion, increasing hydrogen atoms desorbing from the hydride reaction with OH– [19], so the multiphase alloy $La_{0.7}Mg_{0.3}(Ni_{0.9}Co_{0.1})_x$ has a good HRD property.

Fig. 5 shows the low temperature dischargeability of $La_{0.7}Mg_{0.3}(Ni_{0.9}Co_{0.1})_x$ alloys. The LTD can be calculated by the following expression:

$$\text{LTD}\,(\%) = \frac{C_{233}}{C_{293}} \times 100 \quad (2)$$

where C_{233} is the discharge capacity at low temperature 233 K and C_{293} is the discharge capacity at 293 K. It can be seen that the LTD initially increases and then decreases with increasing *x*. At 233 K, the LTD increases from 24.3% ($x = 3.0$) to 58.96% ($x = 3.7$), and then decreases to 48.1% ($x = 3.8$).

Fig. 6 shows discharge capacity versus cycle number of the $La_{0.7}Mg_{0.3}(Ni_{0.9}Co_{0.1})_x$ alloys. After 100 cycles, the retention of the discharge capacity of the alloy electrodes increases from 63.8% ($x = 3.0$) to 93.5% ($x = 3.5$). As compared with the reported value for the same type alloys [21,22], the alloy cycling stability was improved obviously, which is very beneficial to its practical application. The alloy with $x = 3.5$ showed the most suitable electrode properties in terms of capacity and durability, because $La_{0.7}Mg_{0.3}(Ni_{0.9}Co_{0.1})_{3.5}$ alloy contained more stacking-structured phases. The AB_5 phase has relatively low capacity, while the AB_2 phase has relatively larger volume expansion during hydrogen absorption and shows rapid cycle degradation. In the stacking structures of the AB_5 and AB_2 units, it is assumed that volume expansion of the AB_2 unit in the *a*-axis direction is reduced compared to that of the AB_2 phase, and that hydrogen storage capacity is larger than the total capacity of the AB_5 and AB_2 phases, because large amount of hydrogen is absorbed not only inside the AB_2 units but also between the AB_5 and AB_2 units [4]. It is well known that the surface passivation due to surface oxides or hydroxides and the particle pulverization upon cycling lead to the decay of the discharge capacity [23]. The increase of the cycling stability may result from decreas-

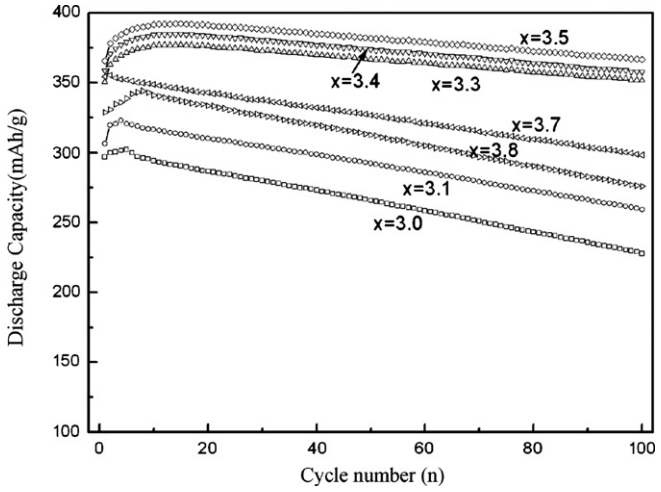

Fig. 6. Discharge capacity versus cycle number of $La_{0.7}Mg_{0.3}(Ni_{0.9}Co_{0.1})_x$ alloys at 293 K.

ing Mg content. In the alkaline KOH aqueous electrolyte Mg can be oxidized to form loose gel-type $Mg(OH)_2$ and the newly formed $Mg(OH)_2$ cannot prevent the alloy from further corrosion. The OH^- can penetrate into the bulk of the alloy particles, attack the fresh surface of the alloy and new hydroxide $Mg(OH)_2$ is formed [24]. The oxidation of alloy particles in the electrolyte leads to a reduction of the amount of active materials and thus a capacity deterioration [21]. A systematic optimization in the value of x may lead to an alloy with high discharge capacity and good cycle stability.

4. Conclusions

In this paper, the hydrogen storage alloy $La_{0.7}Mg_{0.3}(Ni_{0.9}Co_{0.1})_x$ were prepared, and the effects of stoichiometry (x) on the phase structure, the main electrochemical properties of the alloys were investigated. Some conclusions can be summarized as follows:

(1) X-ray diffraction, optical microscopy and energy dispersive spectrometry analyses indicate that the structures of the alloys was multiphase, composed of (La, Mg)Ni_3 phase, $LaNi_5$ phase and (La, Mg)$_2Ni_7$ phase. The lattice parameters of the (La, Mg)Ni_3 phase, (La, Mg)$_2Ni_7$ phase and $LaNi_5$ phase decrease monotonously with the increase of the value x.

(2) The electrochemical studies show that the maximum discharge capacity of the alloy electrodes increases from 356.6 mA h g^{-1} (x = 3.0) to 392.1 mA h g^{-1} (x = 3.5) and then decreases to 344.1 mA h g^{-1} (x = 3.8), the HRD of the alloy electrodes increases from 30.1% (x = 3.0) to 56.1% (x = 3.8), the LTD increases from 24.3% (x = 3.0) to 58.96% (x = 3.7), and then decreases to 48.1% (x = 3.8), and after 100 cycles, the retention of the discharge capacity of the alloy electrodes increases from 63.8% (x = 3.0) to 93.5% (x = 3.5) and then decreases to 80.1% (x = 3.8). A systematic optimization in the amount of x of these alloys may lead to an alloy with high discharge capacity and good cycle stability.

Acknowledgement

This work is supported by the Science and Technology Committee of Shanghai (No. 06JC14028)

References

[1] M. Latroche, A. Percheron-Guégan, J. Alloys Compd. 356–357 (2003) 461–468.
[2] H.G. Pan, Y.F. Zhu, M.X. Gao, Y.F. Liu, R. Li, Y.Q. Lei, Q.D. Wang, J. Alloys Compd. 370 (2004) 254–260.
[3] D.L. Sun, T. Kiyobayashi, H.T. Takeshita, N. Kuriyama, C.M. Jensen, J. Alloys Compd. 337 (2002) L8–L11.
[4] T. Ozake, M. Kanemoto, T. Kakeya, Y. Kitano, M. Kuzuhara, M. Watada, S. Tanase, T. Sakai, J. Alloys Compd. 446–447 (2007) 620–624.
[5] Y.F. Liu, H.G. Pan, M.X. Gao, H. Miao, Y.Q. Lei, Q.D. Wang, Int. J. Hydrogen Energy 33 (2008) 124–133.
[6] Z. Zhang, S.M. Han, Y. Li, T.F. Jing, X.T. Wang, J. Alloys Compd. 421 (2006) 289–293.
[7] Y.G. Yan, Y.G. Chen, H. Liang, C.L. Wu, M.D. Tao, J. Alloys Compd. 427 (2007) 110–114.
[8] M. Latroche, A. Percheron-Guégan, Y. Chabre, J. Bouet, J. Pannetier, E. Ressouche, J. Alloys Compd. 231 (1995) 537–545.
[9] Y.F. Liu, H.G. Pan, M.X. Gao, Y.Q. Lei, Q.D. Wang, J. Alloys Compd. 403 (2005) 296–304.
[10] Y.J. Chai, K. Sakaki, K. Asano, H. Enoki, E. Akiba, T. Kohno, Scr. Mater. 57 (2007) 545–548.
[11] S. Yasuoka, Y. Magari, T. Murata, T. Tanaka, J. Ishida, H. Nakamura, T. Nohma, M. Kihara, Y. Baba, H. Teraoka, J. Power Sources 156 (2006) 662–666.
[12] T. Konhno, H. Yoshida, F. Kawashima, T. Inaba, I. Sakai, M. Yamamote, M. Kanada, J. Alloys Compd. 311 (2000) L5–L7.
[13] T. Yamamoto, H. Inui, M. Yamaguchi, K. Sato, S. Fujitani, I. Yonezu, K. Nishio, Acta Mater. 45 (12) (1997) 5213–5221.
[14] K. Kadir, T. Sakai, I. Uehara, J. Alloys Compd. 302 (2000) 112–117.
[15] Y. Li, S.M. Han, J.H. Li, X.L. Zhu, L. Hu, Mater. Chem. Phys. 108 (2007) 92–96.
[16] H.G. Pan, Y.F. Liu, M.X. Gao, Y.Q. Lei, Q.D. Wang, J. Electrochem. Soc. 150 (2003) A565–A570.
[17] H.G. Pan, Y.F. Liu, M.X. Gao, Y.F. Zhu, Y.Q. Lei, Int. J. Hydrogen Energy 28 (2003) 1219–1228.
[18] Y.H. Zhang, G.Q. Wang, X.P. Dong, S.H. Guo, J.M. Wu, X.L. Wang, J. Alloys Compd. 379 (2004) 298–304.
[19] R. Tang, L.Q. Liu, Y.N. Liu, G. Yu, Int. J. Hydrogen Energy 28 (2003) 815–819.
[20] Y. Sakamoto, K. Kurumq, Y. Naritomi, B. Bunsenges, Phys. Chem. 96 (1992) 1813.
[21] X.P. Dong, Y.H. Zhang, F.X. Lu, L.Y. Yang, X.L. Wang, Int. J. Hydrogen Energy 32 (2007) 4949–4956.
[22] H.G. Pan, N. Chen, M.X. Gao, R. Li, Y.Q. Lei, Q.D. Wang, J. Alloys Compd. 397 (2005) 306–312.
[23] J.J.G. Willems, K.H.J. Buschow, J. Less-Common Met. 129 (1987) 13.
[24] N. Kuriyama, T. Sakai, H. Miyamura, I. Uehara, H. Ishikawa, J. Alloys Compd. 202 (1993) 183–197.